Dune Formation

H.J. Herrmann

Departamento de Física, Universidade Federal do Ceará
Campus do Pici, 60451-970, CE, Brazil
(on sabbatical leave from ICP, University of Stuttgart)
hans@icp.uni-stuttgart.de

Abstract. Dunes are ubiquitous and exist in many forms in deserts and along coasts. They are a consequence of the wind moving sand grains by a mechanism called "saltation". In order to describe the formation and evolution of dunes one must understand the surface flux of sand. Using the equation of motion of turbulent air in the approximation of Jackson and Hunt for gentle hills one obtains a set of equations for dune motion. These equations reproduce very well field measurements. They also allow to study in detail the collision of dunes and the stability of dune fields since their solution is many orders of magnitude faster that real time observations.

1 Introduction

We all know the beautiful landscapes formed by dunes as for instance seen in Figure 1. They are a consequence of the forces exerted on the grains by the wind and the resulting particle flux. The first to systematically study airborne sand transport was the British brigadier R. Bagnold who, during the time of World War II did experiments in wind channels and field measurements in the Sahara. He presented the first expression for the sand flux as function of the wind velocity. Since then more refined expressions have been proposed. Bagnold also described for the first time the two basic mechanisms of sand transport: saltation and creep, and wrote the classic book on the subject which still is consulted very much [1].

If the ground is covered by sand and has no vegetation the sand flux on the surface modifies the shape of the landscape and spontaneously creates patterns on different scales: ripples in the range of ten to twenty centimeters and dunes in the range of two to two hundred meters. The change of the topography can be described by a set of coupled equations of motion which contain as variable fields the shear stress of the wind and the sand flux. These equations allow to explain among others the different dune morphologies, their velocity and their formation.

In this article we will first introduce the properties of the turbulent wind field, then present the mechanisms of sand transport and then we will discuss dune formation.

Fig. 1. Typical desert landscape showing the characteristic sharp edges separating the slip faces from wind driven regions.

2 The wind

Air is a Newtonian fluid of density $\rho = 1,225\text{kgm}^{-3}$ and has a dynamic viscosity $\mu = 1.78 \times 10^{-5}\text{kgm}^{-1}\text{s}^{-1}$ which is defined as

$$\tau = \mu \frac{dv}{dz}$$

where τ is a small applied shear stress and $\frac{dv}{dz}$ the resulting velocity gradient. Its state is fully described by the velocity field $\mathbf{v}(\mathbf{r})$ and the pressure field $p(\mathbf{r})$ when we assume constant temperature and density. Its time evolution is given by the Navier-Stokes equations and the incompressibility condition. The solution of this equation is mainly characterized by the dimensionless Reynolds number defined through

$$Re = \frac{Lv}{\nu}$$

where $\nu = \frac{\mu}{\rho}$ is the kinematic viscosity. L and v are a characteristic length and a characteristic velocity of the problem as it could be given by the boundary conditions. Re represents the ratio of inertial forces to viscous forces. For low Reynolds numbers the flow is laminar. For high Reynolds numbers the flow is turbulent which means that there are strong spatial and temporal fluctuations

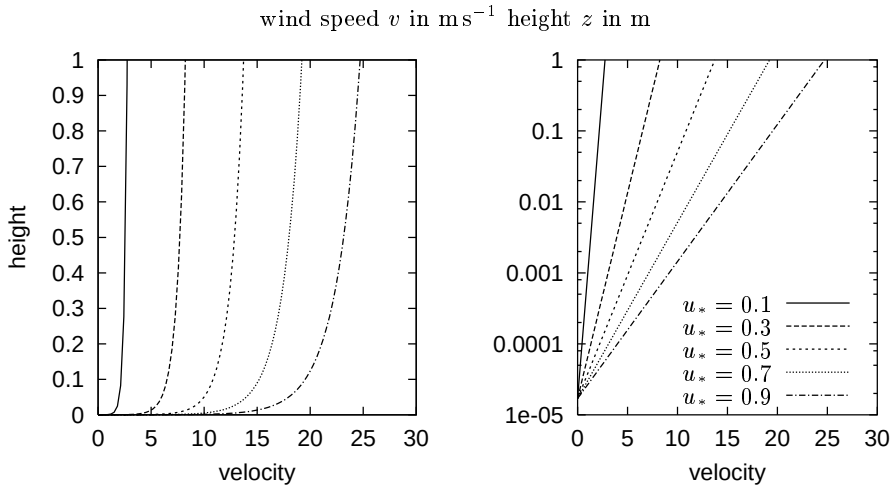

Fig. 2. Velocity profile of the atmospheric boundary layer above a surface with a roughness length $z_0 = 1.7\ 10^{-5}$ m; left: linear scale, right: semi-log plot.

on different scales all the time. This situation is typical outdoor even at moderate wind velocities due to the enormous size of the atmosphere. This complex behaviour arises from the fact that for large Re the Navier-Stokes equation is dominated by the non-linear inertia term.

The critical Reynolds number at which the atmospheric boundary layer becomes turbulent is in the order of 6000 [2].Using the mixing length theory of Prandtl [4] one obtains the well known logarithmic profile of the atmospheric boundary layer illustrated in Figure 2.

$$v(z) = \frac{u_*}{\kappa} \ln \frac{z}{z_0}, \tag{1}$$

where z_0 denotes the roughness length of the surface and $u_* = \sqrt{\tau/\rho}$ the shear velocity. The shear velocity u_* characterizes the flow and has the dimensions of a velocity, although it is actually a measure of the shear stress. The roughness length z_0 is either defined by the thickness of the laminar sublayer for aerodynamically smooth surfaces or by the size of surface perturbations for aerodynamically rough surfaces.

The spatial and temporal fluctuations can be of small scale and high frequency and therefore it is generally too expensive to simulate them directly in practical applications. Instead, the Navier Stokes equations can be time–averaged or ensemble–averaged, or otherwise manipulated to remove the small scale dynamics, which results in a modified set of equations that are computationally more accessible.

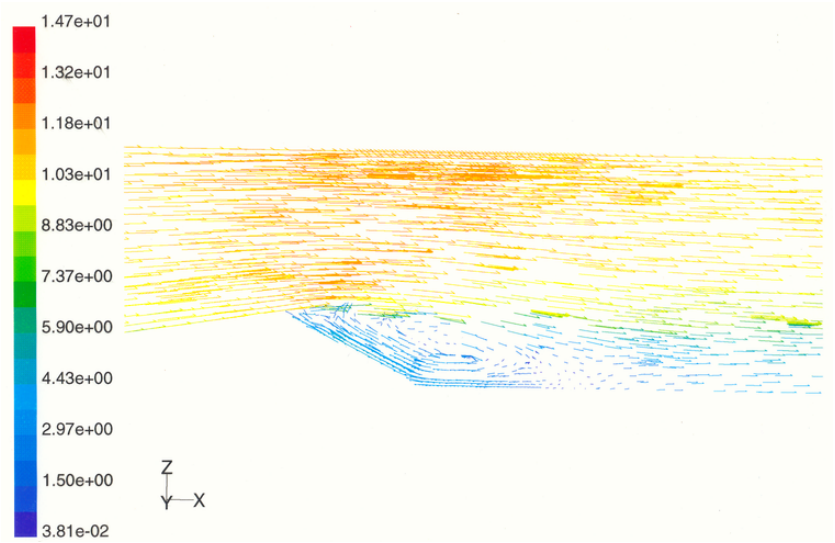

Fig. 3. Velocity field in a longitudinal cut along the central slice of a Barchan dune. One clearly sees the flow separation and a large eddy that forms in the wake of the dune.

One of these approaches for turbulence is the semi–empirical standard k-ϵ model [6] which is based on transport equations for the turbulent kinetic energy k and its dissipation rate ϵ. In the derivation of the k-ϵ model one assumes that the flow is fully turbulent, and the effects of molecular viscosity are negligible.

There are many programs, packages, and libraries available that have been developed to solve the turbulent Navier Stokes equation with different boundary conditions using the k-ϵ model. Nevertheless, three–dimensional turbulent flow on large scales is still a challenge and limited by the performance of processors and memory. We have chosen here the commercial code FLUENT V5.0 [7].

We show in Figure 3 the velocity field of the wind over a crescent-shaped obstacle which is in fact the topography of a real Barchan dune (see Figure 6) measured in Marocco. We see from the cut in wind direction Figure 3 that behind the dune an eddy of relatively low velocity is formed while the strong wind seems to follow above an imaginary continuation of the initial hill following the line $s(x)$ that delimits the eddy (separation line).

The three dimensional calculations using FLUENT are very time consuming from a computational point of view. It is not possible to use it in an iterative calculation as needed to follow the evolution of a dune where the surface and thus the boundary evolves in time. Furthermore, the theoretical understanding is limited by using such a "black–box" model.

A dune or a smooth hill can be considered as a weak modification of the surface that causes a perturbation of the air flow. An analytical calculation of the

shear stress perturbation due to a two dimensional hill has been performed first by Jackson and Hunt [8]. Later, the work has been extended to three dimensional hills and further refined [9–13]. After a rather lengthy calculation they obtain for the Fourier transformation of the shear stress perturbation $\hat{\tau}_x$ in wind direction,

$$\hat{\tau}_x(k_x, k_y) = A \frac{h(k_x, k_y) k_x}{\sqrt{k_x^2 + k_y^2}} \left(k_x + iB|k_x|\right), \tag{2}$$

where $|k| = \sqrt{k_x^2 + k_y^2}$, $\gamma = 0.577216$ (Euler's constant) and A and B depend logarithmically on $\ln L/z_0$.

The non-local convolution integral term is a direct consequence of the pressure perturbation over the hill. The second local term is a correction that comes from the non–linearity of the Navier Stokes equation and represents the effect of inertia. The calculation of the shear stress of the air onto a smooth surface using eq. (2) is computationally very efficient. The limitation of this analytical formula is that it can only be used for surfaces with slopes having less than 30 degrees.

One way to treat this problem of flow separation is to divide the flow into two parts by the separating streamline $s(x)$ that reaches from the brink at which one has the flow separation to the ground.

The area enclosed by the separating streamline and the surface, called the *separation bubble*, a re–circulating flow develops,whereas the (averaged) flow outside is laminar as shown in Figure 3. The general idea, suggested by ref. [10], is that the air shear stress $\tau(x)$ on the windward side can be calculated using the envelope that comprises the dune and the separation bubble Figure 4. In Figure 4 we see the streamline calculated using FLUENT for a test dune that is modelled by a circle segment and a brink position ten meters before the maximum of this circle segment [14]. The dotted line is a fit using an ellipse segment.

3 Sand transport

Sand consists of grains with diameters d which range from $d \approx 2\,\mathrm{mm}$ for very coarse sand to $d \approx 0.05\,\mathrm{mm}$ for very fine sand. The sand itself is mostly composed of quartz ($Si0_2$) which has a density ρ_{quartz} of $2650\,\mathrm{kg\,m^{-3}}$. Dune sand has a quite sharply peaked distribution of diameters because the transport produces a natural mechanism of size segregation.

One can also distinguish sand grains with respect to their shape [15]. An moving fluid such as air exerts a *drag force* F_d which acts in the direction of the flow. For turbulent flow it scales quadratically with the velocity due to Newton's drag law:

$$F_d = \beta \rho u_*^2 \frac{\pi d^2}{4}, \tag{3}$$

where β is a phenomenological parameter. Gravity and inertia oppose the aerodynamic forces. Be $\rho' = \rho_{\mathrm{quartz}} - \rho_{\mathrm{air}}$ the reduced density of the sand grains

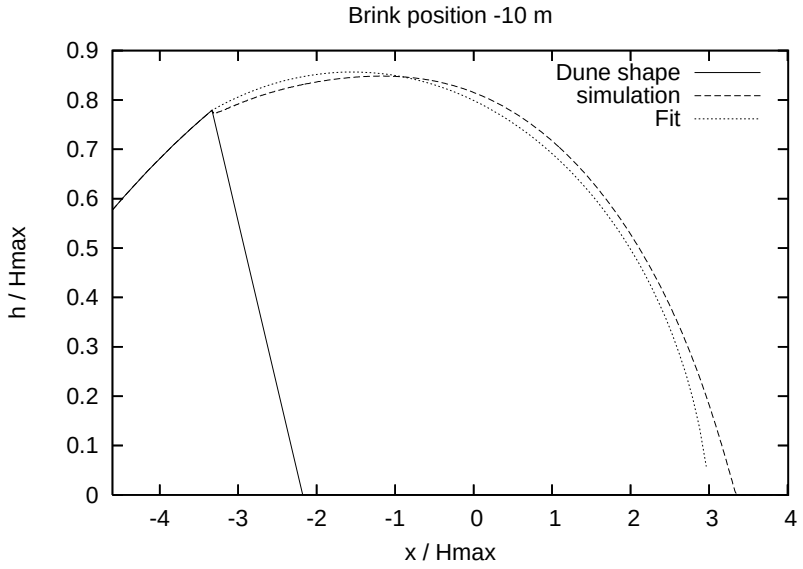

Fig. 4. Separation streamline as calculated with FLUENT (dashed line) and elliptic fit (dotted line) for a dune with a brink position ten meters before the maximum (from ref. [14]).

in the air and the minimal shear stress required to move a grain called *aerodynamic entrainment threshold* $\tau_{ta} = \rho_{\rm air} u_{*ta}^2$. This aerodynamic entrainment fluid threshold shear stress τ_{ta} on a flat surface is directly proportional to the reduced density ρ' and the diameter d of the grains. Shields [17] introduced a dimensionless coefficient Θ that expresses the ratio of the applied tangential force to the inertial force of the grain,

$$\Theta(Re_*) \equiv \frac{\tau_{ta}}{\rho' g d}. \tag{4}$$

Ref. [1] used the dimensionless Shields parameter Θ to define the fluid threshold shear velocity u_{*ta},

$$u_{*ta} = \sqrt{\Theta \frac{\rho' g d}{\rho_{\rm air}}}. \tag{5}$$

This expression is only valid as long as cohesive and adhesive forces can be neglected and thus for grain diameters larger than 0.2 mm. The typical value for the fluid threshold shear velocity $u_{*ta} = 0.25\,{\rm m\,s^{-1}}$ is obtained for $d = 250\,\mu$m using $\Theta = 0.012$.

During sediment transport when sand grains are flying in the air, they impact onto the bed. The momentum transfer from an impacting grain to grains resting on the ground lowers the threshold for entrainment. This has already been observed by Bagnold [18] who called this lowered threshold *impact threshold* u_{*t}.

The impact threshold shear velocity u_{*t} can be calculated in an analogous way and expressed by eq. (5) replacing the Shields parameter by an effective value $\Theta_{eff} = 0.0064$.

Different mechanisms of aeolian sand transport such as suspension and bed–load can be distinguished according to the degree of detachment of the grains from the ground. Bed–load transport can further be divided into saltation, reptation, and creep. Small grains are suspended in air and can travel long distances on irregular trajectories before reaching again the ground.

Saltation is the most relevant bed-load mechanism transport mechanism. To initiate saltation some grains have to be entrained directly by the air. This is called *direct aerodynamic entrainment*. The entrained grains are accelerated by the wind along their trajectory mainly by the drag force before they impact onto the bed again. The interaction between an impacting grain and the bed is called *splash process* and can produce a jet of grains that are ejected into the air. It is currently the subject of theoretical and experimental investigations [19, 20]. Finally, the momentum transferred from the air to the grains gives rise to a deceleration of the air. Due to this negative feedback mechanism saltation reaches a constant transport rate after some transient time.

Using again FLUENT it is possible to calculate the saltation layer on the grain level and obtain the loss of velocity of the wind due to the negative feedback for different heights as done in ref. [27]. An example is given in Figure 5 were we see that the velocity loss occurs mostly around a specific height, namely the one which is typical for the grain trajectories. One also notices that the loss is proportional to the amount of transported grains given through the particle flux q as illustrated in the inset.

When already flying in the air, aerodynamic forces and gravity act on the grain and determine its trajectory [1, 22–24]. The trajectory is close to that of a simple ballistic trajectory. More elaborate calculations [23, 26] have shown that the simple approximation using the ballistic formula gives values which are overstimated by 10–20%.

Measurements performed in wind tunnels [28, 29] show that sand flux starts at a threshold u_{*t} and scales with the cube of the shear velocity ($q \propto u_*^3$) for high shear velocities ($u_* \gg u_{*t}$). In the vicinity of the threshold the functional dependence is not well understood and empirical and theoretical flux relations differ considerably. In fact recent calculations using FLUENT yield a quadratic dependence of the form $q \propto (u_* - u_{*t})^2$ [27]. The simplest flux relation that predicts a cubic relation between sand flux q and shear velocity u_* was proposed by Bagnold [1],

$$q_B = C_B \frac{\rho_{\text{air}}}{g} \sqrt{\frac{d}{D}} u_*^3, \tag{6}$$

being d the real grain diameter and $D = 250\,\mu$m a reference grain diameter. Later the threshold u_{*t} was incorporated into the sand flux relations in order to account for the fact that sand transport cannot be maintained below a certain shear velocity. Many phenomenological sand flux relations have been proposed and have been summarized for instance in ref. [15]. A sand flux relation that is

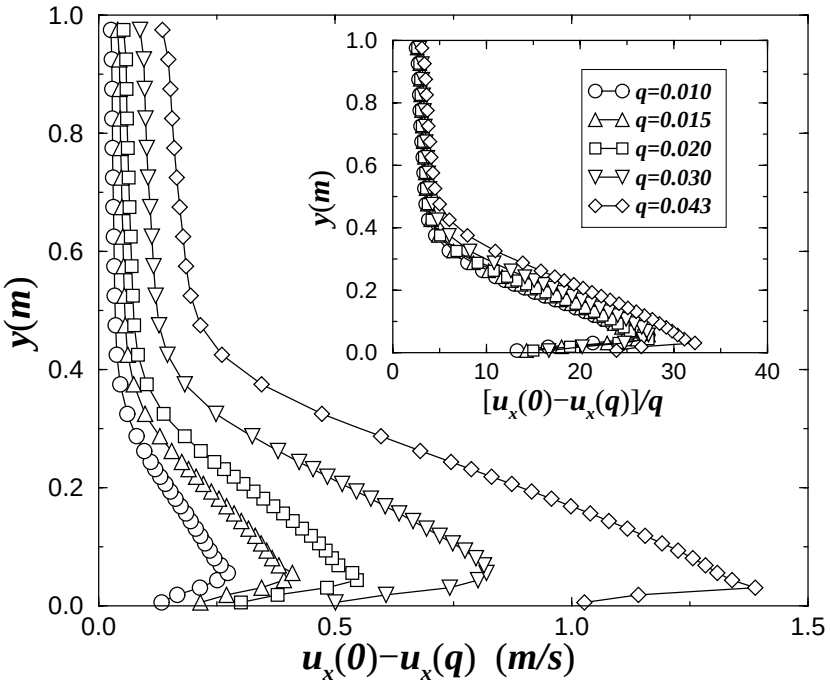

Fig. 5. Profile of the difference of the wind velocity without and with grain transport as function of the height for different fluxes q. The inset shows that this velocity loss scales with q (from ref. [27]).

widely used is the one by Lettau and Lettau [30],

$$q_L = C_L \frac{\rho_{\rm air}}{g} u_*^2 (u_* - u_{*t}) \tag{7}$$

C_L being a fit parameter. Analytical calculations that predict the sand flux by averaging over the microscopic processes have deepened very much the understanding of aeolian sediment transport [22, 23, 31–33].

The relations of the form $q(u_*, ...)$ discused up to now assume that the sediment transport is in steady state, i.e. the sand flux is saturated. In order to overcome this limitation and to get information about the dynamics of the aeolian sand transport, numerical simulations based on the grain scale have been performed [21, 24, 34]. They showed that on a flat surface the typical time to reach the equilibrium state in saltation is approximately two seconds, which was later confirmed by wind tunnel measurements [28].

Assuming that each splash event produces on average the same number of ejected new particles the number of saltating grains would increase exponentially in time. Each accelerated grain, however, removes momentum from the wind

field. Therefore after a saturation time T_s the flux must saturate to a value q_s. From this microscopic picture Sauermann et al.[35–37] have derived an equation describing this evolution of the flux towards saturation

$$\frac{\partial q}{\partial x} = \frac{1}{l_s} q \left(1 - \frac{q}{q_s}\right), \tag{8}$$

l_s being the "saturation length".

Let us emphasize that $T_s(\tau, u)$ and $l_s(\tau, u) = T_s\, u$ are not constant, but depend on the external shear stress τ of the wind and on the mean grain velocity u. We can relate the characteristic time T_s and length l_s of the saturation transients to the saltation time T and the saltation length l of the average trajectory of a saltating grain,

$$T_s = T\,\frac{\tau_t}{\gamma(\tau - \tau_t)}, \qquad l_s = l\,\frac{\tau_t}{\gamma(\tau - \tau_t)} \tag{9}$$

τ_t being the entrainment threshold shear stress and γ a constant. For typical wind speeds, the time to reach saturation is in the order of 2 s [21, 24, 34]. Assuming a grain velocity of 3–5 $\mathrm{m\,s^{-1}}$ [25] we obtain a length scale of the order of 10 m for saturation. This length scale is large enough to play an important role in the formation of dunes.

4 The complete model

The lee side of a hill has the tendency to steepen. If the wind blows long enough from the same direction, the lee side will reach the angle of repose $\Theta \approx 34^o$, which is the steepest stable angle of a free sand surface. If this angle is exceeded, avalanches start to slide down the hill until the surface has relaxed to a slope equal or below the angle of repose. In that case the responsible for sand flux is not the wind but gravity.

Without having to take into account the individual avalanches this effect can be implemented by redistributing the sand in such a way that the slip face is always a straight line with a slope corresponding to the angle of repose Θ. In two dimensions this is easy. In three dimensions this process, however is not straightforward. Bouchaud et al. (BCRE) [38] proposed a set of equations to describe avalanches which allows implementing locally and iteratively even in three dimensions the formation of surfaces having the angle of repose as their steepest inclination. Therefore these BCRE equations seem adequate to describe the dynamics of the slip face.

The complete model is defined by the three variable fields $h(x, y)$, $q(x, y)$ and $\tau(x, y)$. τ is calculated from h through the Fourier transformation of eq. (2). Then q is obtained from τ through eq. (8) using q_s from eq. (7) and l_s from eq. (8). The new topography h is then obtained from q using mass conservation:

$$\frac{\partial h}{\partial t} = \frac{1}{\rho_{\mathrm{sand}}} \nabla_s q \tag{10}$$

Fig. 6. Field of Barchan dunes near Laâyoune, Morocco.

In regions where $\nabla_s h > \tan\Theta$ slip occurs and the just mentioned BCRE equations are applied. ∇_s denotes the spatial derivative in direction of the strongest gradient. Once $h(x,y)$ is obtained one goes back to calculate again $\tau(x,y)$ etc. In this way one iteratively obtains the time evolution of the three fields.

The above system of iteratively solved coupled equations describes fully the motion of the free granular surface under the action of wind and gravity and can be used to calculate formation, evolution and shape of dunes. A natural consequence of the two different driving mechanisms, wind and gravity, is that the solution will separate in two regions: those for which the slope was larger than Θ and where therefore the BCRE equation was applied, ie the slip faces, and those where this was not the case. Theses two regions are separated by characteristic sharp edges which are the typical feature of sandy landscapes as seen in Figure 1.

5 The motion of Dunes

Dunes are land formations of sand of heights, ranging typically from 1 to 500 meters which have been shaped by the wind. These topographical structures are found typically where large masses of sand have accumulated, which can be in the desert or along the beach. Correspondingly one distinguishes desert dunes and coastal dunes. Dunes can be mobile or fixed. Fixed dunes are older and are either "fossilized" which means transformed into a cohesive material, precurser to sand stone, or fixed because the average wind at their site over some period is zero. Otherwise the sand moves if the winds are strong enough, that means typically stronger than 4 meters a second.

As we all know, the beautiful landscapes (Fig. 6) formed by dunes are characterized by very gentle hills interruped by sharp edges called brink lines, delimiting regions of steeper slope, called slip-faces, lying in the wind shadow. Depending on the amount of available sand and the variation of the wind direction, one distinguishes different typical dune morphologies that have been

classified by geographers into over 100 categories. The most well-known are longitudinal, transverse and Barchan dunes; other common dunes are star dunes, ergs, parabolic dunes and draas.

If the wind always comes from the same direction, one obtains transverse dunes if there is much sand and crescent shaped Barchan dunes (from a Turkish word) if little sand is available. Barchans exist in large fields in Marocco, Peru, Namibia etc. as seen in Figure 6). Their velocity ranges from 5 to 50 m per year and is inversely proportional to their height.

An interesting question about Barchans is their shape. In Figure 7 we see a longitudinal cut through the highest point of Barchans of different size normalized in such a way that they all have the same maximum [39].

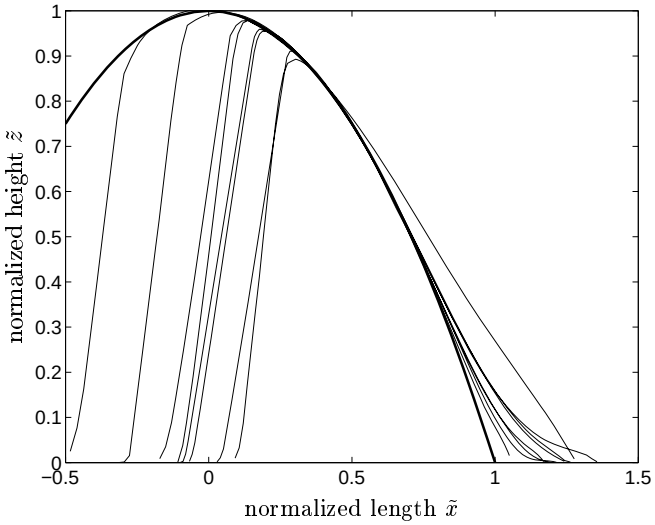

Fig. 7. Longitudinal profiles of eight dunes along their symmetry plane normalizing the length scales such that the shapes collapse on top of each other (from ref. [39]).

On the windward side all curves fall on top of each other, while the crest lies more inwards for increasing dune height. The numerical solution of the equations of the last section reproduced precisely these profiles [40] but on top they do not have the uncontrollable fluctuations that come always from field data. Similarly also the transverse cuts scale with height and the numerical calculation also agrees with the observation.

One consequence of the above similarity relations is a well-known linear dependence between dune height, length and width as has been already reported by Bagnold [1]. Viewing the dune from the top, the brink has the shape of a parabola [39]. Due to the competition between the saturation length and the size of the separation bubble behind the dune one can calculate for the minimal height of a stable dune to be about 1,5 meters. The shear stress of the wind and

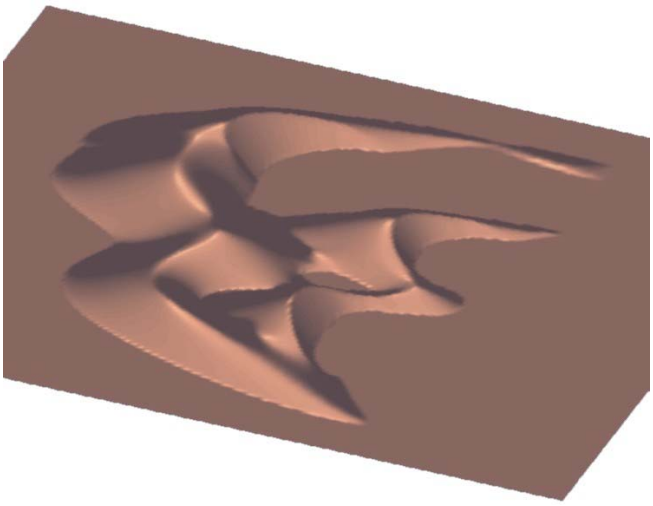

Fig. 8. Complex dune pattern, calculated with the full three dimensional model. Wind is blowing from the left to the right. When Barchan dunes are too close they interact, get eventually connected, and form complex dune structures. The large dunes are shielding the small dunes from the arriving sand flux which then constantly loose volume.

the sand flux on a Barchan dune have also been measured and very favourably been compared to the numerical results of the equations [41].

With these computer dunes it has lately been shown [42] that when a small Barchan bumps into a larger one it can either be swallowed (if it is too small), or it can coalesce but produce at each horn a new baby Barchan (breeding), or it can, if the two initial dunes are of similar size separate again after some exchange of sand (solitary behaviour). In this last case, it looks as if the dunes do cross each other unaltered except for an eventual change in their size.

The system of equations of motion for dunes has also been used to calculate entire systems of dunes and virtual landscapes. An example is shown in Figure 8 where a constant influx of sand is used as boundary condition on the left while on the right one has a free boundary.

6 Conclusion

In this article we have shown that using known expressions for turbulent flow and using the transport mechanism of saltation, it is possible to formulate up a set equations of motion for a wind driven free granular surface. These three coupled equations containing as variable fields the shear stress of the wind, the sand flux at the surface and the profile of the landscape must be complemented by the BCRE equations in regions where the slope exceeds the angle of repose in order to correctly describe the slip faces. The resulting system of equations can be solved iteratively using appropiate boundary conditions and initializations.

The solutions produce patterns that not only ressemble those observed in nature but also agree very well quantitatively with field measurements of shapes, sand fluxes and dune velocities.

The simulation of dune motion on the computer allows make predictions over long time scales since in the real world dune motion is very slow. One can also predict the effect of protective measures like the BOFIX-technique of Meunier [43] and even calculate the dunes on Mars [44]. Recently also the interaction with vegetation has been implemented [45]

References

1. Bagnold, R. A. (1941). *The physics of blown sand and desert dunes.* London: Methuen.
2. Houghton, J. T. (1986). *The physics of atmospheres*, Volume 2nd edn. Cambridge: Cambridge Univ. Press.
3. Kármán, T. (1935). Some aspects of the turbulence problem. *Proc. 4th Int. Congr. Appl. Mech. Cambridge*, 54–91.
4. Prandtl, L. (1935). The mechanics of viscous fluids. In W. F. Durand (Ed.), *Aerodynamic theory*, Volume Vol. III, pp. 34–208. Berlin: Springer.
5. Sutton, O. G. (1953). *Micrometeorology.* New York: McGraw–Hill.
6. Launder, B. E. and Spalding, D. B. (1972). *Lectures in Mathematical Models of Turbulence.* London, England: Academic Press.
7. Fluent Inc. (1999). Fluent 5. Finite Volume Solver.
8. Jackson, P. S. and Hunt, J. C. R. (1975). Turbulent wind flow over a low hill. *Q. J. R. Meteorol. Soc. 101*, 929.
9. Sykes, R. I. (1980). An asymptotic theory of incompressible turbulent boundary layer flow over a small hump. *J. Fluid Mech. 101*, 647–670.
10. Zeman, O. and Jensen, N. O. (1988). Progress report on modeling permanent form sand dunes. *Risø National Laboratory M-2738.*
11. Carruthers, D. J. and Hunt J. C. R. (1990). *Atmospheric Processes over Complex Terrain*, Volume 23, Chapter Fluid Mechanics of Airflow over Hills: Turbulence, Fluxes, and Waves in the Boundary Layer. Am. Meteorological. Soc.
12. Weng, W. S., Hunt, J. C. R., Carruthers, D. J., Warren, A., Wiggs, G. F. S., Livingstone, I. and Castro, I. (1991). Air flow and sand transport over sand dunes. *Acta Mechanica (Suppl.) 2*, 1-22.
13. Hunt, J. C. R., Leibovich, S. and Richards, K. J. (1988). Turbulent wind flow over smooth hills. *Q. J. R. Meteorol. Soc. 114*, 1435-1470.
14. Schatz, V. and Herrmann H.J. (2005). Numerical investigation of flow separation in the lee side of transverse dunes. preprint for Geomorphology.
15. Pye, K. and Tsoar, H. (1990). *Aeolian sand and sand dunes.* London: Unwin Hyman.
16. Chepil, W. S. (1958). The use of evenly spaced hemispheres to evaluate aerodynamic forces on a soil surface. *Trans. Am. Geophys. Union 39*, 397-403.
17. Shields, A. (1936). Applications of similarity principles and turbulence research to bed–load movement. Technical Report Publ. No. 167, California Inst. Technol. Hydrodynamics Lab. Translation of: Mitteilungen der preussischen Versuchsanstalt für Wasserbau und Schiffsbau. W. P. Ott and J. C. van Wehelen (translators).
18. Bagnold, R. A. (1937). The size–grading of sand by wind. *Proc. R. Soc. London 163*(Ser. A), 250–264.

19. Nalpanis, P., Hunt, J. C. R. and Barrett, C. F. (1993). Saltating particles over flat beds. *J. Fluid Mech. 251*, 661–685.
20. Rioual, F., Valance, A. and Bideau, C. (2000). Experimental study of the collision process of a grain on a two–dimensional granular bed. *Phys. Rev. E 62*, 2450–2459.
21. Anderson, R. S. (1991). Wind modification and bed response during saltation of sand in air. *Acta Mechanica (Suppl.) 1*, 21–51.
22. Owen, P. R. (1964). Saltation of uniformed sand grains in air. *J. Fluid. Mech. 20*, 225–242.
23. Sørensen, M. (1991). An analytic model of wind-blown sand transport. *Acta Mechanica (Suppl.) 1*, 67–81.
24. McEwan, I. K. and Willetts, B. B. (1991). Numerical model of the saltation cloud. *Acta Mechanica (Suppl.) 1*, 53–66.
25. Willetts, B. B. and Rice, M. A. (1985). Inter-saltation collisions. In O. E. Barndorff-Nielsen (Ed.), *Proceedings of International Workshop on Physics of Blown Sand*, Volume 8, pp. 83–100. Memoirs.
26. Anderson, R. S. and Hallet, B. (1986). Sediment transport by wind: toward a general model. *Geol. Soc. Am. Bull. 97*, 523–535.
27. Almeida, M.P., Andrade Jr, J.S. and Herrmann, H.J. (2005). Aeolian transport layer. *Phys.Rev.Lett.* in print, cond-mat/0505626.
28. Butterfield, G. R. (1993). Sand transport response to fluctuating wind velocity. In N. J. Clifford, J. R. French, and J. Hardisty (Eds.), *Turbulence: Perspectives on Flow and Sediment Transport*, Chapter 13, pp. 305–335. John Wiley & Sons Ltd.
29. Rasmussen, K. R. and Mikkelsen, H. E. (1991). Wind tunnel observations of aeolian transport rates. *Acta Mechanica Suppl 1*, 135–144.
30. Lettau, K. and Lettau, H. (1978). Experimental and micrometeorological field studies of dune migration. In H. H. Lettau and K. Lettau (Eds.), *Exploring the world's driest climate*. Center for Climatic Research, Univ. Wisconsin: Madison.
31. Ungar, J. E. and Haff, P. K. (1987). Steady state saltation in air. *Sedimentology 34*, 289–299.
32. Sørensen, M. (1985). Estimation of some eolian saltation transport parameters from transport rate profiles. In O. E. B.-N. et al. (Ed.), *Proc. Int. Wkshp. Physics of Blown Sand.*, Volume 1, Denmark, pp. 141–190. University of Aarhus.
33. Werner, B. T. (1990). A steady-state model of wind blown sand transport. *J. Geol. 98*, 1–17.
34. Anderson, R. S. and Haff, P. K. (1988). Simulation of eolian saltation. *Science 241*, 820.
35. Sauermann, G., Kroy K. and Herrmann H. (2001), A continuum saltation model for sand dunes. *Phys. Rev. E 64*, 31305.
36. Kroy, K., Sauermann G. and Herrmann H. J. (2002), A minimal model for sand dunes. *Phys. Rev. Lett. 88*, 054301.
37. Kroy K., Sauermann G. and Herrmann H. J. (2002), Minimal model for aeolian sand dunes *Phys. Rev. E 66*, 31302
38. Bouchaud, J. P., Cates, M. E., Ravi Prakash J., and Edwards S. F. (1994). Hysteresis and metastability in a continuum sandpile model. *J. Phys. France I 4*, 1383.
39. Sauermann, G., Poliakov, A., Rognon, P. and Herrmann, H. J. (2000), The shape of the Barchan dunes of southern Marocco, *Geomorphology 36*, 47-62.
40. Schwämmle, V. and Herrmann, H. J. (2003). A model of Barchan dunes including lateral shear stress, *EPJE 16*, 591-594.

41. Sauermann G., Andrade J. S., Maia L. P. Costa U. M. S., Araújo A. D. and Herrmann H. J. (2003), Wind velocity and sand transport on a Barchan dune, *Geomorphology 1325*, 1-11.
42. Schwämmle V. and Herrmann H. J. (2003), Budding and solitary wave behaviour of dunes *Nature 426*, 619-620.
43. Meunier J. and Rognon P. (2000), Une méthode écologique pour détruire les dunes mobiles, *Secheresse 11*, 309-316.
44. Ribeiro Parteli E.J., Schatz V. and Herrmann H.J. (2005), Barchan dunes on Mars and on Earth, *Powders and Grains 2005*,eds. R. Garcia-Rojo, H.J. Herrmann and S. McNamara (Balkema, Leiden, 2005), p.959-962.
45. Duran O. and Herrmann H.J. (2005) Dune mobility competing with vegetation, submitted to Nature